DOI : https://doi.org/10.56452/0125
ISSN: 0974-5823 Vol. 6 (Special Issue, Nov.-Dec. 2021)
International Journal of Mechanical Engineering

Magnetic and Optical Investigations of PPY/BaFeTiO Nano-composite

Aparna.A.R [a*], Brahmajirao.V [b], Rammohan Y.S [c], Chethana.K.Y [d]

[a*] Department of Aerospace Engineering, BMS College of Engineering, Bengaluru, India

[b] Department of Nanoscience and Technology, GVPCE(Autonomous), Madhurawada,, Visakhapatnam, JNTUK, India

[c] HOD, Department of Aerospace Engineering, BMS College of Engineering, Bengaluru, India

[d] Department of Aerospace Engineering, BMS College of Engineering, Bengaluru, India

Abstract – In this work, optical and magnetic properties of PPY/$BaFe_{(12-x)}Ti_xO_{19}$ hybrid nanocomposite which was prepared in two phases are presented. In the first phase, $BaFe_{(12-x)}Ti_xO_{19}$ (Ti-doped barium ferrite) nanomaterial was synthesized using sol-gel route[3] and in the second phase, $BaFe_{(12-x)}Ti_xO_{19}$ which was synthesised in the first phase, is combined with PPY(polypyrrole) using impregnation technique[1] to prepare a hybrid nanocomposite. Final products obtained are sample1 (PPY/$BaFe_{11.65}Ti_{0.35}O_{19}$ at 850ºC), sample2 (PPY/$BaFe_{11.65}Ti_{0.35}O_{19}$ at 900ºC), and sample3 (PPY/$BaFe_{11.65}Ti_{0.35}O_{19}$ at 950ºC) respectively. The Saturation Magnetisation and crystallite size increased for all samples except for sample2 (PPY/$BaFe_{11.65}Ti_{0.35}O_{19}$ at 900ºC). For all prepared samples, lower squareness ratio indicate formatiom of multi-domain structure. In case of sample 2, the average crystallite size which is a function of temperature and dopant concentration has reduced. Spectroscopic investigations exhibited that the band gap value for sample 2 is increased and the wavelength is shifted. Again for sample3, band gap value is reduced.

Keywords - Barium Ferrite, Polypyrrole, Titanium Butoxide, Magnetic Properties, Optical Properties.

1.0 INTRODUCTION

An easiest tool in the hands of an interceptor is electromagnetic radiation, which is used to deprave the working of an electronic devices in flight vehicles. Many attempts are done in order to make use of the ideal attributes of Nano materials by combining them with many different combinations for electromagnetic interference shielding. In order to protect the working of the device from being tampered by microwave [1-3], a suitable coating material must be used.

Recently, semiconductor-compound Nano crystals of the types of

- Doped Perovskites [15, 16] or
- Doped ferrites [4-14],
- Nanocomposites with one or both of (1) and (2) are assuming importance for this purpose [17,18].

The interactive prospect and chemical stability with the microwave radiation can be obtained by combining the corresponding properties of doped nanoferrites as fillers with matrix of intrinsic conducting polymers like polymethylmethaacrylate , polyaniline, polypyrrole and polyisobutylene [33-38]. This paper presents a new aspect to the above mentioned task by synthesizing PPY/$BaFe_{12-x}Ti_xO_{19}$ [19] nanocomposite material and carrying out various characterization techniques on as prepared samples.

Author [19] reported the data of FTIR, SEM and XRD of these materials and EDS, TEM, HISTOGRAM and SAED in [20]. This work is recognized to be the first in the literature by the Sci – finder software. Results showed that the Ti- doped barium ferrite ($BaFe_{11.65}Ti_{0.35}O_{19}$) nano powders has been successfully incorporated into polypyrrole nanocomposite.

2.0 EXPERIMENTAL METHOD

2.1 Preparation of samples are done in two phases

Phase 1: Ferrite preparation

Here three different solutions were prepared based on the composition of $BaFe_{12-x}Ti_{(x)}O_{19}$ (x = 0.35)[19] . In order to obtain a clear solution (1), metal ferrite is dissolved into deionized water along with an appropriate amount of citric acid and stirred for 30 minutes. In order to prepare solution (2), dissolve specific amounts of Ti(OC4H9)4 and citric acid in absolute ethyl alcohol by stirring for 30 minutes until it becomes clear. During three hours, the mixture was continuously stirred as the solution (2) was added very slowly to solution (1). This resulted in a clear Solution (3). The pH value of Solution (3) was then lowered by adding ammonia drop by drop, until it reached 7.0. In order for the gel to form and for combustion to begin, acidity will be necessary in order to maintain a clear solution and to prevent precipitation of either one or both of the reactants. Standard pH meters were used to measure pH. Nanomaterials are characterized by their properties influenced by the pH. A study found that weight losses were small with an increasing pH, as well as particle size increased [39, 40]. Also, with an increasing pH, particle size was also reported to increase

DOI : https://doi.org/10.56452/0125

[39, 40]. To form viscous sol precursors, the obtained solution has been evaporated at 800 °C and dried for 24 to 48 hours under an oven at 120 °C. The viscous sol was then heated for three hours at various temperatures, 850ºC, 900ºC, and 950ºC. The flow chart of the same has already been published [21].

Phase 2: Preparation of composite

Nano powders containing $BaFe_{(12-x)}Ti_xO_{19}$ (x = 0.35) and polypyrrole were synthesized and mixed with various weight percents of methanol (BFTO powder = 97% and polypyrrole = 3%) to synthesize BFTO/PPY nanocomposite. The mixture was stirred for 2 hours and evaporated for 30 minutes. The mixture is then dried overnight.PPY/$BaFe_{11.65}Ti_{0.35}O_{19}$ at 850ºC and sample 2 (PPY/$BaFe_{11.65}Ti_{0.35}O_{19}$ at 900ºC) are obtained. sample3 PPY/$BaFe_{11.65}Ti_{0.35}O_{19}$ at 950ºC) is obtained from PPY/$BaFe_{11.65}Ti_{0.35}O_{19}$. There is already a detailed flowchart of the same [20].

3.0 RESULTS AND DISCUSSION

Studies of prepared samples using vibration sample magnetometry (VSM) were conducted at the Indian Institute of Technology, Chennai, with a Lakeshore VSM 7410 SET UP. An optical absorption spectrometer (UV-Vis) was used to record the optical absorption spectra of the three samples at CNST, JNTU, Hyderabad in the wavelength range 400- 800 nm at room temperature.

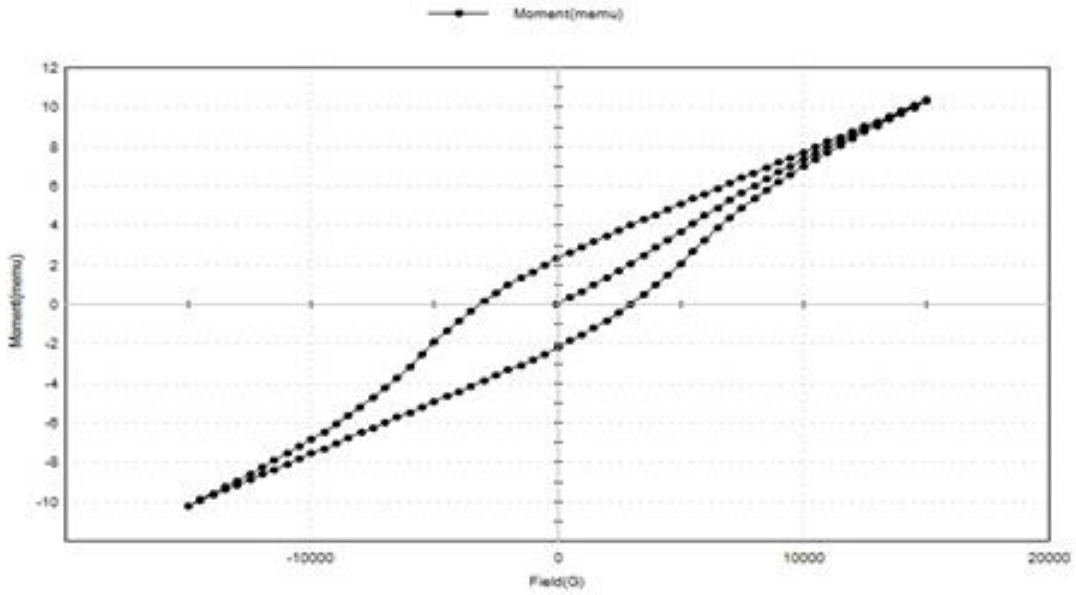

Fig. 1. SAMPLE 1 PPY/ $BaFe_{11.65}Ti_{0.35}O_{19}$ at 850°C

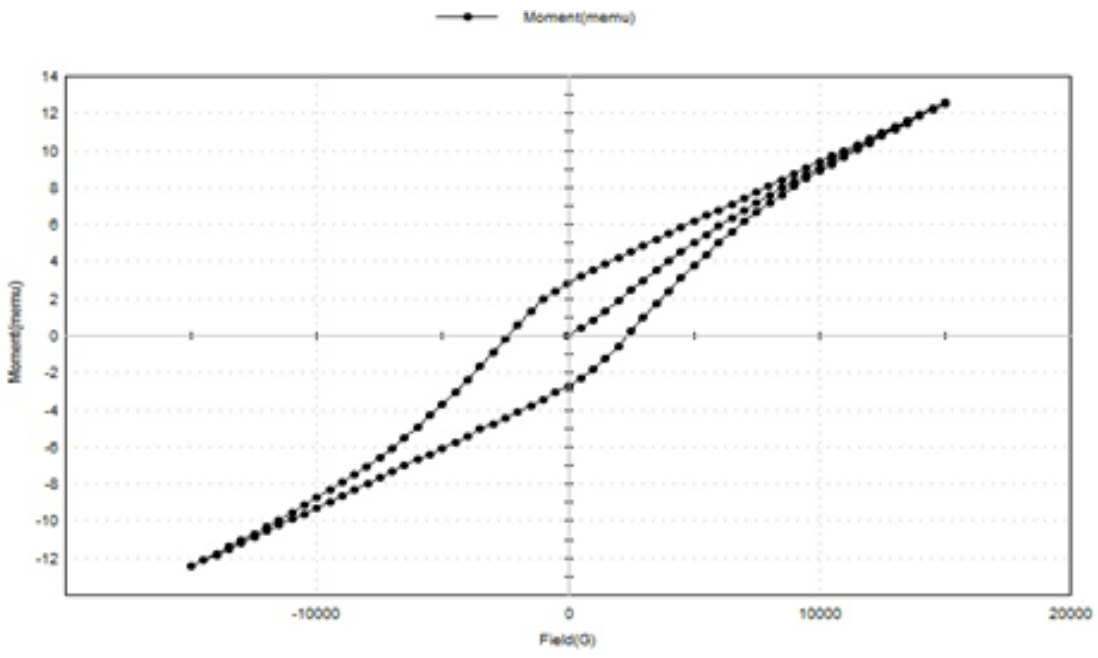

Fig. 2. SAMPLE2 PPY/ $BaFe_{11.65}Ti_{0.35}O_{19}$ at 900°C

DOI : https://doi.org/10.56452/0125

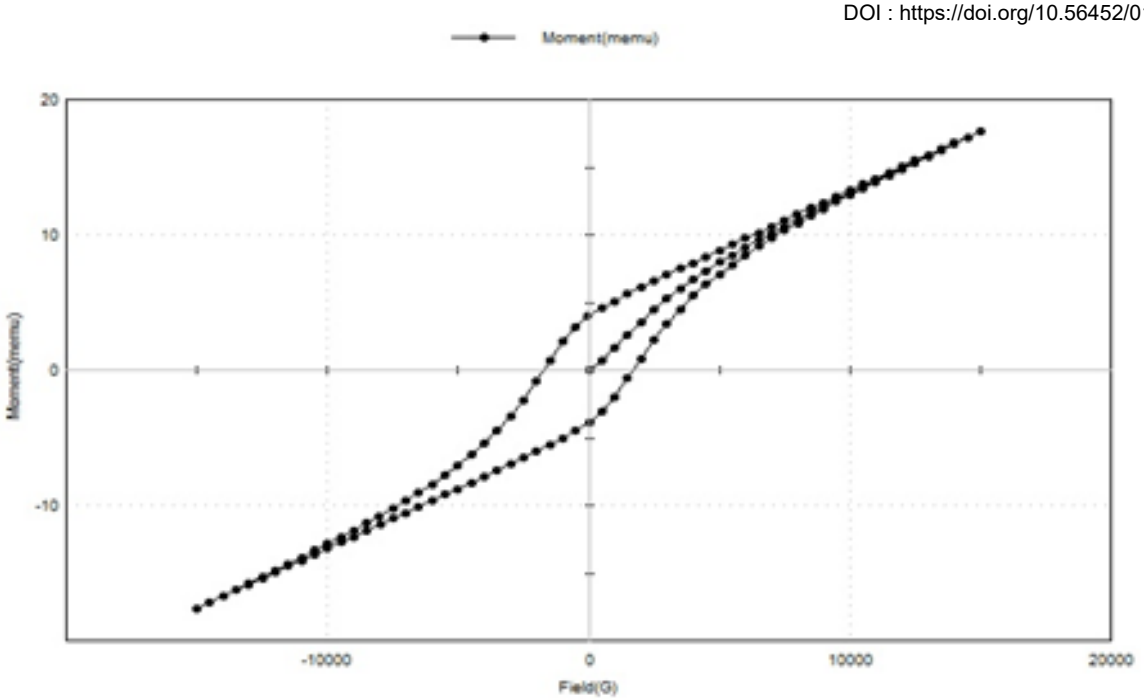

Fig. 3. SAMPLE 3 PPY/ $BaFe_{11.65}Ti_{0.35}O_{19}$@950°C

3.1 Vibration Sample Magnetometry

An embodiment of vibration sample magnetometry at room temperature is shown in fig a, b, and c for a comparison of field-dependent magnetic properties. Magnetic parameters such as coercivity (Hc), saturation magnetisation (Ms), remanent magnetisation (MR), anisotropy constant (K), magnetic moment (Nb), and crystallite size, while M_S^0 marks the points where magnetization holds constant value, are listed in table1.

Because none of the samples reached saturation magnetisation, they all show discrete absence of paramagnetic nature. (M_S^0) indicates the point at which magnetization starts to assume constant value during forward and reverse cycling. The magnetization also increases with increasing field strength (instead of reaching saturation value). Hysteresis loops of all samples exhibit this behavior.

Due to the relatively larger surface area of fine magnetic particles [22], surface chemistry plays a greater role in the magnetic properties of these particles. PPY/$BaFe_{11.65}Ti_{0.35}O_{19}$ at 900°C showed the lowest saturation magnetisation of all samples. When PPY/$BaFe_{11.65}Ti_{0.35}O_{19}$ are heated to 900°C, the number of aligned magnons is less. Sample1 has a high saturation magnetization while sample2 has a reduced saturation magnetization, and sample3 again has a high saturation magnetization. The reason behind this is that sample2 is transitioning at this temperature, which we can call the transition temperature. Therefore, M decreases as well as Saturation Magnetization. For sample 1 and sample 3, saturation magnetization increases due to more magnon aligning in the external field's direction. The result is an increase in magnetic moment.

Maximum saturation magnetization occurs when the temperature is 950°C. The coating material must meet this condition to shield microwave radiation. The size of the crystallites, which is related to dopant concentrations and temperatures, determines the number of particles present in the domain. Ferromagnetism is a result of this, which can be observed in VSM studies. This was already discussed in the earlier XRD study [19] regarding crystallite size and lattice constant. If the size of the domains increases, it indicates that there are more magnons in the domains whereas if the size decreases, it indicates that there are more magnons in sub-lattices that cause ferromagnetism. As the retentivity and coercivity values vary, the magnetic properties of sub- lattices show a variation in ferrites with different doping concentrations and temperatures. The analysis of the measurements of parameters associated with hysteresis loops indicates that all prepared samples form wasp waists. A high level of wasp waistlines is evident for sample3 and the hysteresis loop indicates that wasp waist lines are newly formed. Wasp waist lines appear to be more prevalent in other samples. Multi-domain formation is indicated by lower squareness ratios. No sample reaches saturation in magnetization.

DOI : https://doi.org/10.56452/0125

Table-1 : Hysteresis parameters of PPY/ $BaFe_{12-x}Ti_xO_{19}$ for sample1,sample2 and sample3

Sample	H_c (oe)	M_R emu/ gm	M_S emu /gm	M_R / M_S	K X10^4 Ergs/cm3	Nb X10^2	M_s^o	Avg.crystallite size
PPY/ $BaFe_{11.65}Ti_{0.35}O_{19}$ at 850°C	3075.7	0.070721	0.3209	0.2203	493.38	0.0675	12923*0.285	15.09
PPY/ $BaFe_{11.65}Ti_{0.35}O_{19}$ at 900°C	2376.3	0.066159	0.2979	0.2221	353.9	0.0627	12519* 0.256	13.303
PPY/ $BaFe_{11.65}Ti_{0.35}O_{19}$ at 950°C	1720.5	0.074166	0.3326	0.223	286.03	0.0699	11223* 0.2606	18.26

3.2 UV-Visible Spectrophotometer

A Shimadzu spectrometer (model UV-3100), operated at room temperature, was used to measure optical absorption spectra for the samples at CNST, JNTU, Hyderabad.

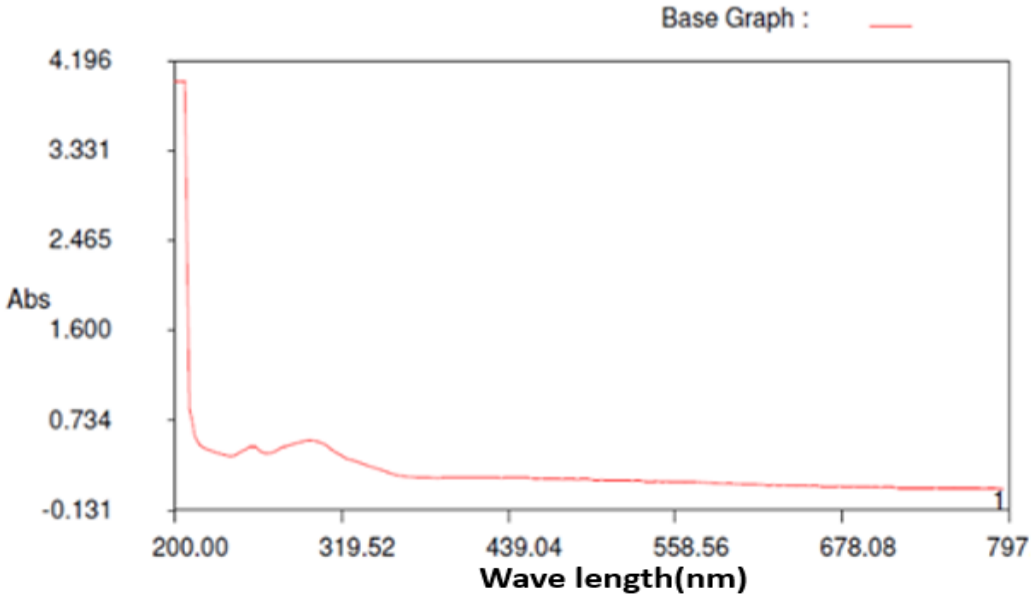

Fig 4. Sample 1 PPY/ $BaFe_{11.65}Ti_{0.35}O_{19}$ at 850°C

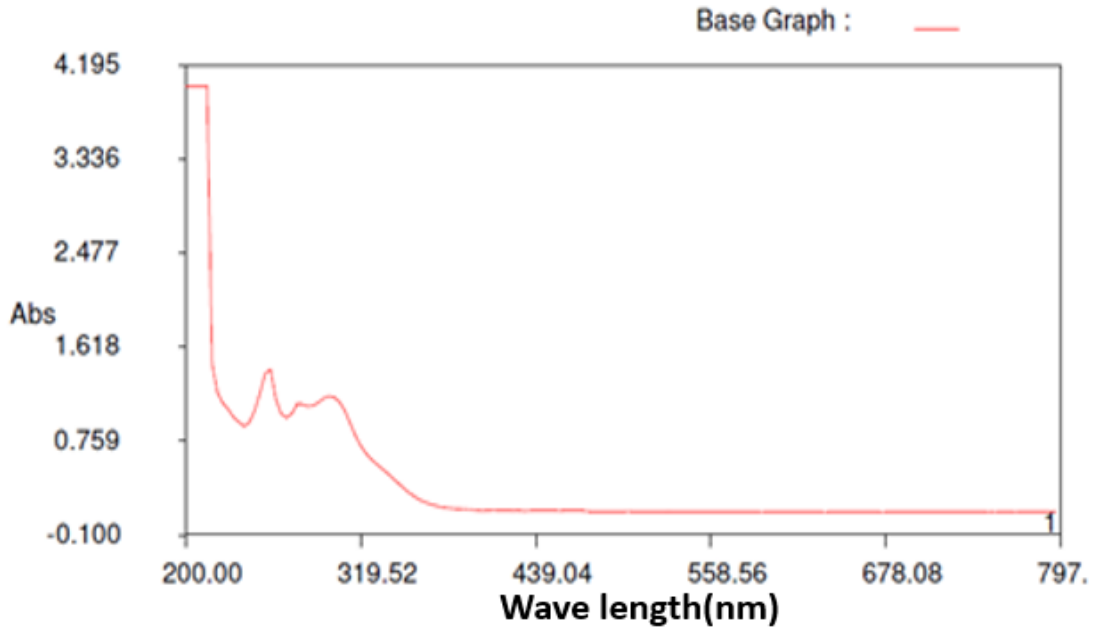

Fig. 5. Sample 2 PPY/ $BaFe_{11.65}Ti_{0.35}O_{19}$ at 900°C

DOI : https://doi.org/10.56452/0125

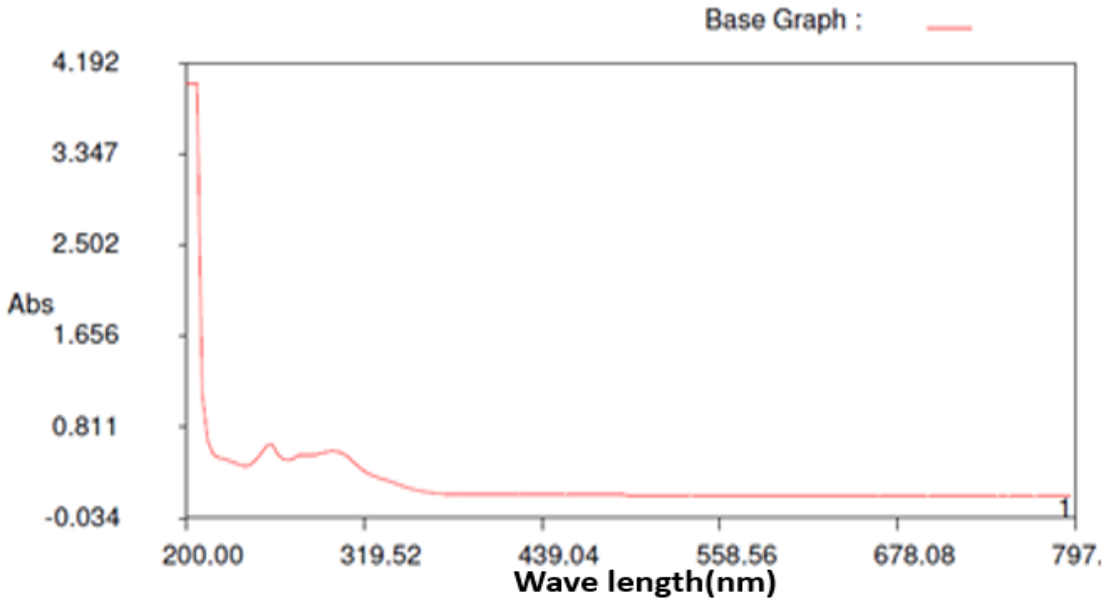

Fig. 6. Sample 3 PPY/ $BaFe_{11.65}Ti_{0.35}O_{19}$ at 950°C

Analyzing Tauc plots for nano composites to determine Band Gap values. Band gap values are reported in the literature for pure barium hexaferrite at 3.79ev [23] and pure polypyrrole at 1.37ev [43]. The graph illustrates the change in band gap as a function of the sintering temperature. Nano-regime quantum confinement is credited with the increase in band gap value [28]. Increased band gap is a consequence of quantum confinement at the nanoscale.PPY/ $BaFe_{12-x}Ti_xO_{19}$ nanocomposite is analyzed to determine its band gap. LCMT (ligand to metal charge transfer) produces one peak around *250 nm, whereas PPY incorporation into nanoferrite at many different temperatures has another peak around *290 nm. At the three temperatures that we tested, 850ºC, 900ºC, and 950ºC, we found two peaks that confirm the proper formation of PPY/BaFeTiO19 nanocomposites.

Sample-2 showed an increased band gap value, whereas sample3 had a decreased band gap and its wavelength shifted. Agrain boundaries, crystalline defects, and dislocations further contribute to the absorption of light in the longer wavelength region [25]. Due to this, sample 3 does not exhibit an absorption peak around 250nm. In addition, sample 3 lacks an absorption peak around 250nm because of its cation distribution [29] and decreased band gap due to increased crystallite size, along with increased temperature due to decreased band gap. Upon considering that the amplitude of atomic vibrations increases with the increase in thermal energy, this behavior becomes more understandable [30]. The effect of an increasing interatomic spacing is to reduce the electron's potential, thereby decreasing the energy band gap of the material [31]. Further, by increasing the temperature of the sintering to 950ºC, remanent magnetization (M_R) increased (see the results in Table 1). As shown by the variation in M_R with calcination temperature, if oxygen vacancies were decreased, this would result in improved super exchange interactions between Fe3þ– O2– Fe3þ, originating from three parallel and two antiparallel sub-lattices (2a, 12k and 2b), thereby improving the nanomaterial's ferromagnetic properties [32].

Table-2 : Absorption peak and also the band gap values of PPY/ $BAFE_{12-X}Ti_XO_{19}$PPY/ $BAFE_{12-X}Ti_XO_{19}$

Sample	Absorption around ~250nm	Absorption around ~270nm	Absorption around ~290nm	E_g (ev)
PPY/$BaFe_{11.65}Ti_{0.35}O_{19}$ at 850ºC	253.65	277.71	296.72	5.36
PPY/$BaFe_{11.65}Ti_{0.35}O_{19}$ at 900ºC	257.01	272.82	298.75	5.39
PPY/$BaFe_{11.65}Ti_{0.35}O_{19}$ at 950ºC	-	280.40	298.91	5.20

4.0 CONCLUSION

All characterization techniques carried out on the prepared samples proved that the $BaFe_{12-x}Ti_xO_{19}$ has been successfully incorporated into the PPY polymer. Magnetic and optical studies on the prepared samples are carried out by utilizing standard characterization methods. UV-VIS spectroscopy was used to measure band gap of prepared samples and hysteresis loop studies were conducted using VSM technique. Our magnetic properties topological model correlated with wasp-waist formation while studying VSM. Paleomagnetic studies have discussed this mechanism for a long time[6]. For this work, the Nobel Prize has been awarded in 2016. The field in the longitudinal direction of the wire is oscillatory and uniform in an anisotropic easy-plane magnetic wire, Aharonov developed an analysis of the soliton-anti-soliton interaction. Wasp waists observeable in hysteresis loops are sufficiently formed by this. A synthesised PPY/BaFeTiO nanocomposite can be used for absorbing microwave radiation as a coating on stealth fighters, so radars cannot detect the aircraft [41] and the synthesised material also has conductive properties with an

DOI : https://doi.org/10.56452/0125
improved impedance matching, so the material provides higher absorption capacity [42,35]. Considering this, In light of this, we plan to conduct Mossbauer studies, ac and dc conductivity studies, dielectric studies, and Raman impact studies for the purposes of future demonstrations.

ACKNOWLEDGMENT

The Authors are appreciative to the division of Nanoscience and Technology CNST, JNTU, Hyderabad, DST SAIF, IIT Madras and Sophisticated Analytical Instrumental Facility, Cochin for their assistance to do the portrayal of tests.

REFERENCES

[1] Mu G, Pan X, Chen N, He C, Gu M, Synthesis and characterization of hard magnetic composites-Hollow microsphere/ titania /barium ferrite, Appl. Surf. Sci. 254(2008) 2483-2486.
[2] Wang C, Han X, Xu P, Wang X, Li X, Zhao H, Magnetic and dielectric properties of barium titanate-coated barium ferrite. J. Alloy Compd. 476(2009) 560-565.
[3] Li Y, Wang Q, Yang H . Synthesis, characterization and magnetic properties on nanocrystalline BaFe12O19. Curr. Appl. Phys. 9(2009).
[4] Xiuna Chen et.al,(2012) "Multiferroic Properties of BaFe12O19 Ceramics" (13) < arxivweb.arxiv.org/list/cond-mat.mtrl-sci/1201?skip=10&show>.Phys. Rev. B 85, 115439 (2012).
[5] Kojima, H.(1982) 'Fundamental Properties of Hexagonal Ferriteswith Magnetoplumbite Structure' , Handbook of Ferromagnetic Materials; Elsevier: Amsterdam, 1982; Vol. 3, pp305_391.
[6] Tsung-Shune, C. (2000), 'Permanent Magnet Films for Applications in Microelectromechanical Systems', J. Magn. Magn.Mater.2000, 209, pp75–79.
[7] Nakamura, Het.al.,(1987), 'Cobalt-Titanium Substituted Barium FerriteFilms for Magneto-Optical Memory', J. Appl. Phys. 1987, 61, pp3346–3348.
[8] Uher, J.et.al., (1991), 'Tunable Microwave and Millimeter-Wave Band-Pass Filters', IEEE Trans. Microwave Theory Tech.1991, 39, pp 643–653.
[9] Jalli, J.et.al,(2009), 'Growth andCharacterization of 144 μm Thick Barium Ferrite SingleCrystalline Film for Microwave Device Application', J. Appl.Phys. 2009, 105, p07A511. 1375-1380.
[10] G. Yang, B. Han, Z. Sun, L. Yan, X. Wang, Preparation and characterization of brown nanometer pigment with spinel structure, Dyes Pigments 55 (2002) 9–16.
[11] Y.A. Koksharov, D.A. Pankratov, S.P. Gubin, I.D. Kosobudsky, M. Beltran, Y.Khodorkovsky, A.M. Tishin, Electron paramagnetic resonance of ferrite nanoparticles, J. Appl. Phys. (2001), 89 (4) , pp 2293–2298.
[12] T. Fujiwara, Magnetic-properties and recording characteristics of barium ferrite media, IEEE Trans. Magn. (1987) , 23 ,p3125.
[13] V. Berbenni, A. Marini, N.J. Welham, P. Galinetto, M.C. Mozzati, The effect of mechanical milling on the solid state reactions in the barium oxalate–iron(III) oxide system, J. Eur. Ceram. Soc. 23, (2003),pp 179–187.
[14] K. Haneda, A.H. Morrish, Magnetic properties of small particles for possible magneto-optical pigments, IEEE Trans. Magn. (1999), 35, pp 3490–3495.
[15] Nakamura, Het.al.,(1987), 'Cobalt-Titanium Substituted Barium FerriteFilms for Magneto-Optical Memory', J. Appl. Phys. 1987, 61, pp3346–3348.
[16] Jingguo Jia, Chuyang Liu, Ning Ma, Gaorong Han,WenjianWeng and Piyi Du, Exchange coupling controlled ferrite with dual magnetic resonance and broad frequency bandwidth in microwave absorption, Sci.Technol. Adv. Mater. 14 (2013), pp 1-8.
[17] Ping Xu, Xijiang Han, Chao Wang, Hongtao Zhao, Jingyu Wang, Xiaohong Wang and Bin Zhang. Synthesis of Electromagnetic Functionalized Barium Ferrite Nanoparticles Embedded in Polypyrrole. J Phys Chem B 2008;112: 2775-2781.
[18] M.S. Kim, et.al., , Synth. Met. 126 (2002) 233–239.
[19] Aparna.A.R., V. Brahmajirao and T.V.Karthikeyan, Synthesis and Characterization Study of Polypyrrole Composite of Titanium Doped Barium Ferrite ($Bafe_{(12-x)}$ Ti_xO_{19}), International Journal of Engineering Research and Development (IJERD), Volume 12, 2016,PP.18-23.
[20] Aparna.A.R., V. Brahmajirao and T.V.Karthikeyan, Incorporation of ($Bafe_{(12-x)}$ Ti_xO_{19}), into conducting polymer and their characterisation study, IOSR Journal of Electronics and Communication Engineering (IOSR-JECE,Volume 12, Issue 1, Ver. I (Jan.-Feb. 2017), PP 43-45.
[21] Aparna.A.R., V. Brahmajirao , T.V.Karthikeyan, and Dr.Moneesha Fernandes, Synthesis and Structural, Morphological & FTIR Studies on Ferrite Powders Bafe (12−X) Ti Xo 19, Using Sol-Gel Method, IOSR Journal of Applied Physics (IOSR-JAP), Volume 8, (Jan. –Feb. 2016), PP 18-26.
[22] Yavuz, O¬.; Ram, M. K.; Aldissi, M.; Poddar, P.; Hariharan, S. J.Mater. Chem. 2005, 15, 810.
[23] T. Kaur et al, Enhancement in physical properties of barium hexaferrite with Substitution, J. Mater. Res., 1-10 2015.
[24] L. Tauxe , Paleo magnetic Principles and Practice, 2006.https://books.google.co.in/books?isbn=0306481286.
[25] V.S. Shanthala et.al., optical band gap studies of polypyrrole doped with cuznfe2o4 nano particles, International Journal of Scientific and Research Publications, Volume 6, Issue 9, September 2016
[26] Aharonov ,Bohm Transport and Topological Effects in Graphene Molecular Junctions and Graphene Nanorings Constantine Yannouleas, J. Phys. Chem. C119,2015,pp. 11131−11142. DOI:10.1021/jp511934v
[27] Jingguo Jia, Chuyang Liu, Ning Ma, Gaorong Han, Wenjian Weng and Piyi Du, Exchange coupling controlled ferrite with

dual magnetic resonance and broad frequency bandwidth in microwave absorption, Science &Technology of Advanced Materials, IOP Publishing,vol. 14, 2013,pp.4

[28] Aparna.A.R., V. Brahmajirao and T.V.Karthikeyan, Magnetic, optical and thermal studies of PPY/$BaFe_{12-x}Ti_xO_{19}$ nanocomposite, International Journal of Engineering Research and Development (IJERD)Volume 13, Issue 1 (January 2017), PP.11-18.

[29] Butembu Sabastine[1] et al., Optical and scanning kelvin probe microscopic characterization of sol-gel synthesized aluminum doped zinc cobalt ferrite nanoparticles, International Journal of Physical Sciences, Vol. 15(4), pp. 151-161, October-December, 2020

[30] L. Mino, G. Agostini, E. Borfecchia, D. Gianolio, A. Piovano, E. Gallo, C. Lamberti, Low-dimensional systems investigated by x-ray absorption spectroscopy: a selection of 2D, 1D and 0D cases, J. Phys. D: Appl. Phys. 46 (2013) 42300142–42300172.

[31] B. van Zeghbroeck, Principles of semiconductor devices, third ed., USA, 2011.

[32] I. Sharifi, H. Shokrollahi, M. Doroodmand, R. Safi, Magnetic and structural studies on CoFe2O4 nanoparticles synthesized by co-precipitation, normal micelles and reverse micelles methods, J. Magn. Magn. Mater. 324 (2012) 1854–1861

[33] Saini P. et al. Electromagnetic interference shielding behavior of polyaniline/graphite composites prepared by in situ emulsion pathway.J. Appl. Polym. Sci. 113, 3146 (2009).

[34] Joo J. et al. Electromagnetic radiation shielding by intrinsically conducting polymers. J. Appl. Phys. Lett.65, 2278 (1994).

[35] Wang Y. et al. Intrinsically conducting polymers for electromagnetic interference shielding.Polym.Adv.Technol. 16, 344 (2005).

[36] Chung D. D. L. et al. Electromagnetic interference shielding effectiveness of carbon materials. Carbon 39, 279 (2001).

[37] B. Birs¨oz, A. Baykal, H. S¨ozeri, and M. S. Toprak, ―Synthesis and characterization of cpolypyrrole-BaFe12O19 nanocomposite,‖Journal of Alloys and Compounds, vol. 493, no. 1-2, pp.481–485, 2010.

[38] C. Zhang, Q. Li, and Y. Ye, ―Preparation and characterization of polypyrrole/nano-SrFe12O19 composites by in situ polymerization method,‖ Synthetic Metals, vol. 159, no.11, pp. 1008–1013, 2009.

[39] Praveena K, Sadhana K, Srinath S and Murthy SR. Effect of pH on structural and magnetic properties of nanocrystalline Y3Fe5O12 by aqueous co-precipitation method. Material Research Innovations 2013;18:69-75.

[40] Kim T , Nasu S and Shima M. Growth and magnetic behavior of bismuth substituted yttrium iron garnetnanoparticles. Journal of Nanoparticle Research 2007; 9(5): 737-743.

[41] Michael Green, Anh Thi Van Tran, Xiaobo Chen, Maximizing the microwave absorption performance of polypyrrole by data-driven discovery, Composites Science and Technology, 10.1016/j.compscitech.2020.108332, (108332), (2020).

[42] Ali Motamedi, Roohollah Rahmanifard, Morteza Adibi, Synthesis and microwave absorption characteristics of

BaFe12O19/BaTiO3/MWCNT/polypyrrole quaternary composite, Synthetic Metals, 10.1016/j.synthmet.2021.116873, 280, (116873), (2021).

[43] V.S. Shanthala , S.N. Shobha Devi , M. V. Murugendrappa optical band gap studies of polypyrrole doped with cuznfe2o4 nano particles, International Journal of Scientific and Research Publications, Volume 6, Issue 9, September 2016 21 ISSN 2250-3153